J Mater Sci (2008) 43:1818–1824
DOI 10.1007/s10853-007-2397-9

Transient bleaching pulse shapes in electrochromic polysiloxane thin films

David Mitchell Goldie

Received: 12 November 2007 / Accepted: 10 December 2007 / Published online: 18 January 2008

Abstract Transient bleaching currents are examined for a series of electrochromic carbazole-modified polysiloxane thin films. The shape of the bleaching currents is found to be sensitive to the type of counter-ion employed and the initial density of counter-ion charge that is deposited in the films during the colouration stage. Pure space-charge-limited (SCL) transport of counter-ions that posses a well-defined mobility is inconsistent with the observed pulse shapes and a modified SCL model that involves fast and slow mobility sites is proposed. The modified SCL model may describe a variety of transient bleaching pulse shapes (including current overshoots) as charge is removed from the electrochromic films and the counter-ions are constrained to transfer from slow to fast discharge sites.

Introduction

Thin-film materials that exhibit electrochromic behaviour offer potentially important commercial opportunities for low information content displays [1–3] and glazings on windows and mirrors [1–5]. Important materials in this respect include tungsten trioxide (WO_3) where considerable effort has focussed upon understanding the dynamics of electronic and ionic charge transport in an attempt to achieve acceptable response times for display applications [6]. For WO_3 based electrochromic systems, the colouration and bleaching processes respectively involve the introduction and removal of counter-ions (H^+) from the film bulk to form a tungsten bronze H_xWO_3. The dynamics of the counter-ion interactions within the WO_3 lattice are well understood and the associated colouration and bleaching currents were successfully modelled [7–9]. Thin-film alternatives to WO_3 include organic polymer materials with appropriate side groups which function as colour centres when placed in an appropriate oxidation state [10, 11]. Electrochromic phenomena in these materials also depend upon the presence of counter-ions but, unlike WO_3, the dynamics of colouration and bleaching exhibit unique properties that present new challenges to model. A good example is provided by carbazole-modified polysiloxane (CMP) materials which exhibit electrochromic behaviour when cross-linked to produced dicarbazyl colour centres [12]. Previous work with this system [13–16] has established that the dependence of observed bleach times upon the bleaching potential were entirely consistent with a simplified bleach model developed for WO_3 films [8]. However, certain aspects of the associated transient bleach pulses, such as current overshoots, cannot be explained using the WO_3 bleach model. The present work is therefore concerned with evaluating how the WO_3 bleach model may be realistically modified to account for the rich variety of bleach pulses found in CMP films when either the type of counter-ion, or the initial concentration of counter-ions in the film, is varied.

Experimental details

The growth conditions used to cross-link the CMPs and deposit the electrochromic films was described, elsewhere [12–14]. In all cases the CMP used was poly[3-(carbazolyl-9-yl)propyl]methylsiloxane and the counter-ion during electrochemical growth was hexafluorphosphate (PF_6^-).

D. M. Goldie (✉)
Division of Electronic Engineering and Physics,
University of Dundee, Dundee DD1 4HN, Scotland
e-mail: d.m.goldie@dundee.ac.uk

The films were grown on gold working electrodes and had a measured thickness of 0.8 μm as determined by electron microscopy. Colouration and bleaching of the electrochromic films was conducted using a two-terminal cell configuration that comprised the gold working electrodes and an aluminium counter-electrode in a 0.1 M dichloromethane solution of electrolyte salt [14]. The electrolyte salts used were tetrabutylammonium tetrafluoroborate, tetrabutylammonium perchlorate and tetrabutylammonium hexafluorophosphate to respectively provide a source of BF_4^-, ClO_4^- and PF_6^- counter-ions. Transient currents that arose during the colouration and bleach processes were recorded on a digitising oscilloscope and transferred to a computer for subsequent analysis.

Results and discussion

To commence the study of the bleach mechanism in CMP electrochromic films, the effect of the counter-ion type upon the transient current response was investigated. The results obtained are given in Fig. 1, where for each counter-ion type several current pulses were recorded for applied bleaching voltages (V_b) that range from 0.8 to 2.0 V. In all cases, the films have initially been coloured using identical conditions such that the amount of counter-ion charge in the films $Q_s = 3.5$ mC cm^{-2}. This value for Q_s corresponds very closely to the maximum available density of colouration centres in the films for the applied colouration potential of 2.0 V [13]. Examination of the Fig. 1 data reveals that for all counter-ion types, the transient current responses comprise two distinct regions; a bleach region during which counter-ion charge is continually being removed from the film, and a post-bleach region when counter-ions have been successfully removed and the current decays rapidly to zero. The transition between these current regimes is easily identified for the Fig. 1 curves and allows the bleach time (t_b) to be experimentally determined. As expected the bleach time is seen to reduce as the applied bleach voltage is increased. The dependence of t_b upon V_b was analytically shown to be consistent with [14];

$$t_b = \frac{2Q_s L^3}{9\varepsilon_r \varepsilon_0 \mu_i V_b^2} \quad (1)$$

In Eq. 1, L is the film thickness, ε_r is the permittivity of the electrochromic material, and μ_i is the counter-ion mobility. Previous application of this expression to the Fig. 1 data using an assumed value for $\varepsilon_r = 3$ allowed μ_i for the various counter-ion types to be deduced as given in Table 1. These μ_i values appear reasonable for ionic transport with the slight differences originally ascribed to the relative ease with which different sized counter-ions could move through the cross-linked lattice [14, 16]. It must be appreciated, however, that Eq. 1 is derived from a bleach model originally developed for WO_3 systems that involves a double-extraction mechanism for neutral plasma in the electrochromic film bulk [8]. The basis of this model is depicted in Fig. 2. Adapted for the present CMP system, the interface between the electrochromic film and the

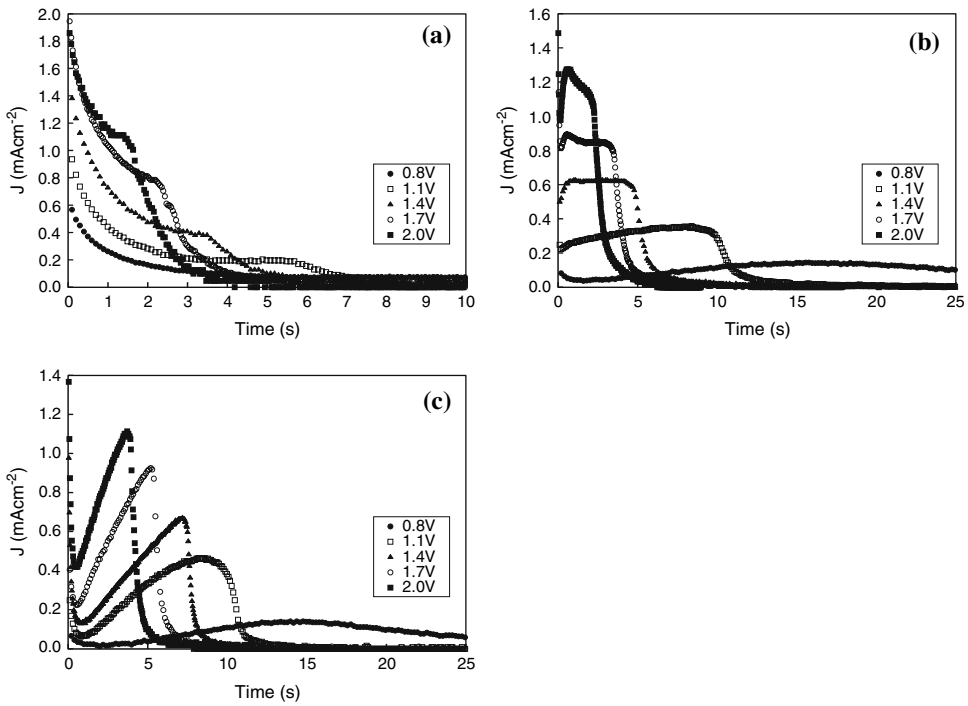

Fig. 1 Bleach currents recorded under ambient room temperature conditions for 0.8 μm thick CMP electrochromic films. The counter-ions are (**a**) BF_4^-, (**b**) ClO_4^- and (**c**) PF_6^-. The bleach voltages applied are given in the inset legends

Table 1 Counter-ion parameters determined using bleach data in CMP electrochromic films

Counter-ion	Relative size[a]	μ_i^b ($cm^2\ V^{-1}\ s^{-1}$)	m^c	μ_L^c ($cm^2\ V^{-1}\ s^{-1}$)	Fast sites (%)
BF_4^-	1.00	2.2×10^{-4}	2.7	4.9×10^{-4}	14
ClO_4^-	1.08	1.8×10^{-4}	3.0	5.4×10^{-4}	14
PF_6^-	1.12	1.1×10^{-4}	3.2	4.3×10^{-4}	13

[a] Ratio of counter-ion size to the BF_4^- size found by molecular modelling

[b] From Eq. 1 taking $\varepsilon_r = 3.0$

[c] Fitted parameters to Eq. 6

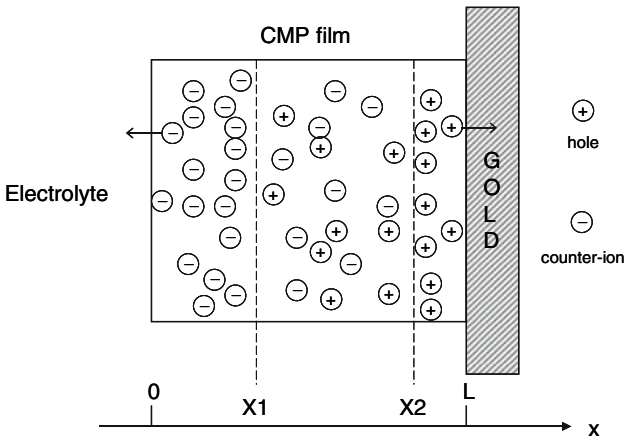

Fig. 2 Schematic geometry of a CMP electrochromic film which shows the important internal regions during the bleach process. The neutral plasma of counter-ions and holes lies between the reference boundary lines marked *X*1 and *X*2

electrolyte is located at $x = 0$ so that the gold electrode is situated at $x = L$ for a film thickness L. Starting from an initially neutral plasma of counter-ions and holes throughout the film following the colouration step at time $t = 0$, the bleaching process is then envisaged to involve the simultaneous extraction from the film of counter-ions into the electrolyte, and holes into the gold electrode. At any time during this bleach period ($t < t_b$), the neutral plasma will extend from $x = X1$ to $x = X2$ as shown in Fig. 2 where $X1$ and $X2$ define the boundary regions in the vicinity of the electrolyte and gold interfaces which are devoid of holes and counter-ions, respectively. As time advances and charge extraction continues, $X1(t)$ will increase whereas $X2(t)$ will decrease until $X1 = X2$ at $t = t_b$ [8]. Assuming that the hole mobility is very much larger than that of the counter-ions, then $X2(t) \approx L$ for the duration of the bleach period. The bleach current is then entirely attributable to the space-charge-limited (SCL) flow of counter-ions in the region $0 < x < X1$. This SCL current is maintained by the effective injection of counter-ions from the neutral plasma as $X1$ increases with time. An analysis of the injection mechanism using standard SCL theory predicts that the bleach current $J_b(t)$ should decay with time according to [8];

$$J_b(t) = \left[\frac{9Q_s^3\varepsilon_0\varepsilon_r\mu_i}{8L^3}\right]^{\frac{1}{4}} \cdot \frac{V_b^{\frac{1}{2}}}{(4t)^{\frac{3}{4}}} \quad \text{for } t < t_b \tag{2}$$

Eq. 2 provides an excellent description for the bleach currents observed in WO_3 films [7, 8]. However, for CMP the $J(t)$ curves presented in Fig. 1 do not follow the universal time decay that is demanded by Eq. 2. In particular, it is noted that $J(t)$ for the CMP films is sensitive to the counter-ion used. A decay of $J(t)$ is only observed for the BF_4^- counter-ion, but the decay is considerably weaker than the $t^{-3/4}$ dependence expected from Eq. 2. By contrast the use of the ClO_4^- counter-ions gives an almost time-independent $J(t)$ response, whereas the PF_6^- counter-ion shows a remarkable increase of $J(t)$ with time. The use of the WO_3 bleach model to describe the CMP bleach currents would therefore appear to be inappropriate despite the fact that this model does explain successfully the associated variation of t_b with V_b through Eq. 1.

In order to evaluate why the WO_3 bleach model is consistent with the CMP data via Eq. 1, yet inconsistent via Eq. 2, it is useful to consider the assumptions and simplifications upon which the model is based. Central to the simplification of the SCL mathematics, the model proposes that the films remain uniformly coloured throughout the film thickness during bleaching. The volume charge density (n) of counter-ions in the SCL region ($0 < x < X1$) is consequently taken to be $n(x) = n_0 = \text{constant}$ where $n_0 L = Q_s$. Furthermore, the mobility of the counter-ions in the SCL region is assumed to have no dependence upon the local electric field (F) or the x-location so that $\mu(F,x) = \mu_i = \text{constant}$. These simplifications might not be appropriate for the CMP films and expressions equivalent to Eq. 1 for t_b, and Eq. 2 for $J(t)$, may be developed when these restrictions are relaxed. For example, as bleaching progresses, the electric field across the SCL region will continually change as $X1$ increases and the volume space charge between 0 and $X1$ diminishes. If the movement of counter-ions through the CMP bulk is sensitive to the electric filed, then this should be accommodated into the SCL model through a field-dependent mobility $\mu(F)$. Additionally, the deposited CMP films may not in reality possess spatial uniformity

throughout the grown thickness. Such non-uniformity might influence the density of colouration centres, and how counter-ions may move through the CMP lattice, and may be incorporated into the SCL model through a spatial dependence of $n(x)$ and $\mu(x)$ respectively. The results of relaxing the WO_3 model simplifications are summarised in Table 2. In Table 2 the underlying functional formats taken for $\mu(F, x)$ and $n(x)$ in the SCL analysis are indicated. Note that to simplify the modified SCL analysis, the actual functional formats taken were in practice simple power laws, so that $\mu(x) = \mu_i(x/L)^\gamma$. The effect of incorporating these functional changes are indicated in the final two columns of Table 2 which consider whether the model changes maintain the observed relationship of t_b upon V_b and permit $J(t)$ to increase with time. It is evident that none of the modified WO_3 SCL models is capable of generating both of the latter requirements. Although the introduction of a spatial aspect into either the mobility or volume space charge maintains the Eq. 1 dependence of t_b upon V_b, it is found that $J(t)$ continues in general to decay with time and may at best be rendered independent of time only if the spatial dependence of $\mu(x)$ or $n(x)$ increases at an unrealistically rapid rate with x. Whilst the SCL_$\mu(x)$ and SCL_$n(x)$ models could therefore in principle account for the BF_4^- and ClO_4^- data in Fig. 1 they are incapable of explaining the PF_6^- results. Only the SCL_$\mu(F)$ model specifically allows $J(t)$ to increase with time as seen for the Fig. 1 PF_6^- curves but introducing an electric field-dependent parameter into the SCL analysis destroys the necessary $t_b \propto V_b^{-2}$ relationship.

It is evident from the above considerations that the entire CMP bleaching properties cannot be explained through subtle modifications to the WO_3 SCL bleach model. Nevertheless, the applicability of Eq. 1 is persuasive for the retention of a bleach model that is controlled by the SCL current flow of counter-ions in the region $0 < x < X1$. To further explore whether such an SCL current may describe the data in Fig. 1, it is important to appreciate that Eq. 2 is founded upon the classic SCL analysis which for the Fig. 2 geometry places the (ohmic) injecting contact at $x = X1$ and the collection contact at $x = 0$. Under these conditions the SCL current J_{SCL} is given by [17];

$$J_{SCL} = \frac{9}{8}\frac{\varepsilon_0 \varepsilon_r \mu_i V_b^2}{X1^3} \tag{3}$$

If it is assumed that the only parameter within Eq. 3 that is time-dependent during the bleach period is $X1$, it follows that $J_{SCL}(t)$ is dictated by $X1(t)$ that depends upon the assumed forms for $n(x)$ and $\mu_i(x)$. For the simplified circumstances where these are assumed constant (model SCL_WO3 in Table 2) we find $X1(t) \propto t^{1/4}$ and so $J(X1(t)) \propto t^{-3/4}$ as given by Eq. 2. Irrespective of the exact form of $X1(t)$, the adoption of the classic SCL expression for J_{SCL} would therefore appear to preclude any possibility that the current might increase since $X1(t)$ must increase as bleaching progresses. However, as $X1(t)$ increases, the associated concentration of counter-ion charge $N(X1)$ that is contained in the CMP film between $x = 0$ and $x = X1$ is set by SCL considerations to be [8, 17];

$$N(X1) = \left(\frac{18}{8}\right)^{\frac{1}{2}} \cdot \frac{\varepsilon_0 \varepsilon_r V_b}{X1} \tag{4}$$

The dynamics of the bleaching process thus demands that, as $X1$ increases, counter-ions are removed from the CMP film to the electrolyte to ensure that the remaining concentration of counter-ions in the SCL region is consistent with Eq. 4. This SCL constraint prompts a re-examination of Eq. 3 to enquire whether any of the parameters that appear may depend upon $X1$ (and hence time) through the accompanying variation of $N(X1)$. The obvious candidate parameter is the counter-ion mobility μ_i where the freedom of movement of counter-ion charge may be sensitive to the overall occupation of colouration centres. In order to investigate this possibility each experimental $J(t)$ bleach curve in Fig. 1 was first used to determine the $X1$ location at around 20 predetermined integration-times τ that spanned the interval $0 < \tau < t_b$. This was accomplished by simple numerical integration of the $J(t)$ curves following a spline-fit such that if the colouration throughout the film thickness is assumed to be uniform;

$$X1(\tau) = \frac{\int_0^\tau J(t)dt}{\int_0^{t_b} J(t)dt} \cdot L \tag{5}$$

Knowing $X1(\tau)$ the variation of μ_i with $X1$, and hence with $N(X1)$, was calculated by applying Eq. 3 to the Fig. 1 curves. The results are shown in Fig. 3 where $\mu_i(X1)$ is plotted against $X1$ on a double-logarithmic scale. For each

Table 2 SCL bleach models considered for the analysis of bleach data in CMP electrochromic films

Bleach model	$\mu(F, x)$[a]	$n(x)$[b]	$t_b \propto V_b^{-2}$[c]	$J(t) \uparrow$[d]
SCL_WO3	μ_i	n_0	✔	×
SCL_μ(F)	$\mu(F)$	n_0	×	✔
SCL_μ(x)	$\mu(x)$	n_0	✔	×
SCL_$n(x)$	μ_i	$n(x)$	✔	×

SCL_WO3 is the standard bleach model for WO_3 electrochromic films. The other models are modified from SCL_W03 and are described in the text

[a] Functional form of mobility in SCL analysis

[b] Functional form of counter-ion charge density in SCL analysis

[c] Does SCL analysis maintain $t_b \propto V_b^{-2}$ dependence?

[d] Does SCL analysis permit $J(t)$ to increase with time?

counter-ion type the data points for various V_b in Fig. 3 appear to lie along a common line which may be modelled by a simple power-law such that;

$$\mu_i(X1) = \mu_L \left(\frac{X1}{L}\right)^m \tag{6}$$

In Eq. 6 μ_L is the counter-ion mobility when $X1 = L$ and m is a constant. Regression fitting using Eq. 6 gives the dashed-lines shown in Fig. 3 from which the parameters μ_L and m in Table 1 are deduced. As anticipated, m has a value of 3 for ClO_4^- since for this counter-ion $J(t)$ is essentially time independent. Compared with ClO_4^- the parameter m assumes a slightly lower value for BF_4^-, and a slightly higher value for PF_6^-, as demanded by $J(t)$ for these counter-ions. Interestingly μ_L appears to have no obvious dependence upon counter-ion type. Using the functional format for $\mu_i(X1)$ suggested by Eq. 6 alternative expressions to Eq. 1 for t_b and Eq. 2 for $J_b(t)$ may subsequently be developed. Provided m is less than 4 in Eq. 6 the modified expressions are found to be;

$$t_b = \frac{8Q_sL^3}{9(4-m)\varepsilon_r\varepsilon_0\mu_L V_b^2} \tag{7a}$$

$$J_b(t) = \left[\frac{9Q_s^{(3-m)}\varepsilon_0\varepsilon_r\mu_L}{8L^3}\right]^{\frac{1}{(4-m)}} \cdot \frac{V_b^{\frac{2}{(4-m)}}}{((4-m)t)^{\frac{(3-m)}{(4-m)}}} \quad \text{for } t < t_b \tag{7b}$$

It is noted that Eq. 7a and b correctly reproduce Eqs. 1 and 2 when $m = 0$ and μ_i is independent of $X1$. Equation 7a therefore maintains the $t_b \propto V_b^{-2}$ relationship with the constant of proportionality now being determined by μ_L and m. The ability of Eq. 7a to successfully calculate experimental bleach times is illustrated in Fig. 4 where $\sqrt{(1/t_b)}$ is plotted against V_b. For each counter-ion type the predicted response is shown as a labelled line which has been generated from Eq. 7a using the appropriate μ_L and m values from Table 2 and using ε_r as a common fitting parameter. The experimental bleach times that are found from the current signals in Fig. 1 are also plotted in Fig. 4 as discrete data points. The agreement between the experimental data and the predicted response is optimised for $\varepsilon_r = 3.8$ which is comparable to the ε_r value found for

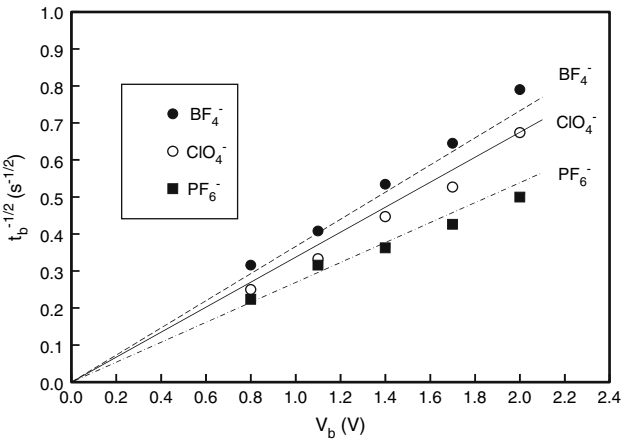

Fig. 4 Comparison of Eq. 7a with bleach times determined from Fig. 1. The experimental bleach times are plotted as discrete points and the predicted responses (generated using $\varepsilon_r = 3.8$) are shown by the labelled lines for the counter-ions indicated

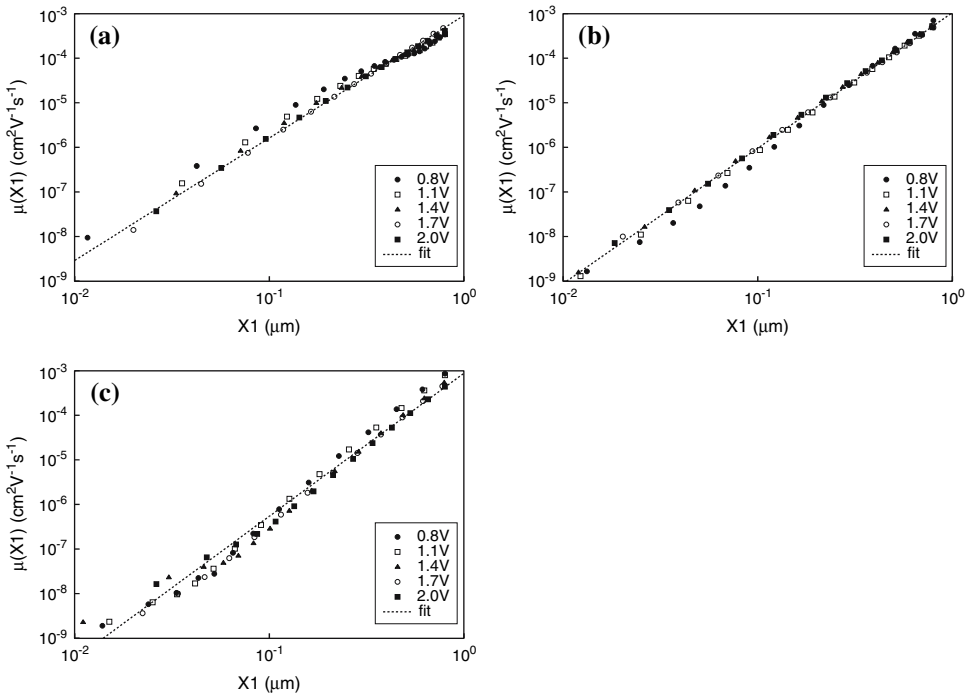

Fig. 3 The experimentally calculated average mobility of counter-ions in the SCL region as a function of $X1$. The counter-ions ions are (**a**) BF_4^-, (**b**) $Cl0_4^-$ and (**c**) PF_6^-. The bleach voltages applied are given in the inset legends, and the dashed lines represent the best power-law fits to the data points

amorphous CMP materials[1] [18]. The proposal that the counter-ion mobility increases as bleaching proceeds according to Eq. 6 is therefore supported by the measured bleach times.

The underlying physical origin of Eq. 6 may originate in how counter-ions are distributed throughout the electrochromic film following the colouration stage. It is suggested that for CMP electrochromic films, the cross-linked structure possesses colouration sites whose speed of access by counter-ions during colouration may be classified as either fast or slow. Fast sites will be occupied in preference to slow sites during the colouration stage so that in general a fully-coloured film will initially contain a charge concentration n_F of fast counter-ions, and a charge concentration n_S of slow counter-ions. During bleaching, the partitioning of the counter-ions into fast and slow centres must comply with the SCL criterion given by Eq. 4 for the total charge concentration $N(X1)$ so that;

$$n_F(X1) + n_S(X1) = N(X1) \tag{8}$$

The favoured removal route for counter-ions during bleaching will take place via the fast sites. At some stage during the bleaching period, counter-ions will therefore be channelled from slow to fast sites as demanded by Eq. 8. If the mobility of counter-ions in fast sites (μ_F) is considerably greater than that for slow sites, the effective counter-ion mobility in the SCL region will be proportional to the fraction of fast to slow charge. Using similar arguments as applied to trap-limited electronic transport in disordered semiconductors [19], $\mu_i(X1)$ may thus be expressed as;

$$\mu_i(X1) = \mu_F \cdot \frac{n_F(X1)}{N(X1)} \tag{9}$$

A comparison of Eq. 9 with the phenomenological expression given by Eq. 6 suggests that the fitting parameter μ_L is equivalent to the mobility μ_F of counter-ions in fast sites. The identification of $\mu_F = \mu_L$ arises from the observation that at the end of the bleach period, $X1 = L$ in Eq. 6 and so $\mu(L) = \mu_L$. Correspondingly, all charge must eventually reside in fast sites to be finally removed which requires $n_F(L) = N(L)$ in Eq. 9 and so $\mu(L) = \mu_F$. As noted earlier, the μ_L values given in Table 1 appear to be insensitive to the counter-ion type. This consistency of μ_L implies that the mobility of fast sites in identically grown CMP films is not influenced by the type of counter-ion used for electrochromic operation. The ease of access to fast sites in the CMP films must therefore be equal for each type of counter-ion used in the present work. By contrast, the access of counter-ions to slow sites would appear to be strongly influenced by the counter-ion type employed as reflected through the parameter m in Table 2. The parameter m essentially indicates the rate at which counter-ions in slow sites may transfer to fast sites to allow bleaching to proceed. The fastest bleaching occurs when $m = 0$ since for this special case all counter-ions occupy fast sites with $\mu_i = \mu_F$. As m increases, bleaching become slower in accordance with Eq. 7a as counter-ions must now transfer between slow and fast sites. The rate of transfer dictates $n_F(X1)$ and $n_S(X1)$ at any stage $X1$ during the bleach period and hence $\mu_i(X1)$ via Eq. 9. For the m values given in Table 2 it would therefore appear that transfer from slow to fast sites is suppressed as the size of the counter-ion becomes larger. Access to the slow sites may consequently be influenced by the physical size of the counter-ion when it encounters specific colouration centre locations.

In order to further test the proposed existence of fast and slow colouration sites in the CMP films, the relative occupation of fast to slow sites at the start of the bleaching process was attempted by controlling the times used to colour the films. It was anticipated that for sufficiently short colouration times, the counter-ions would prefer to populate the more accessible fast sites. The associated $J_b(t)$ response should thus correspond to the featureless decay predicted by Eq. 2 when $m = 0$ in Eq. 7b. However, above a critical colouration time threshold, the available fast sites would become saturated and counter-ions would be forced to occupy the remaining slow sites. The current response should now exhibit some structure according to Eq. 7b with $m > 0$ as counter-ions must transfer from slow to fast sites to permit bleaching. The results obtained from such an investigation are given in Fig. 5 which shows bleaching currents using a PF_6^- counter-ion when the colouration time is varied between 10 and 270 s. For colouration times

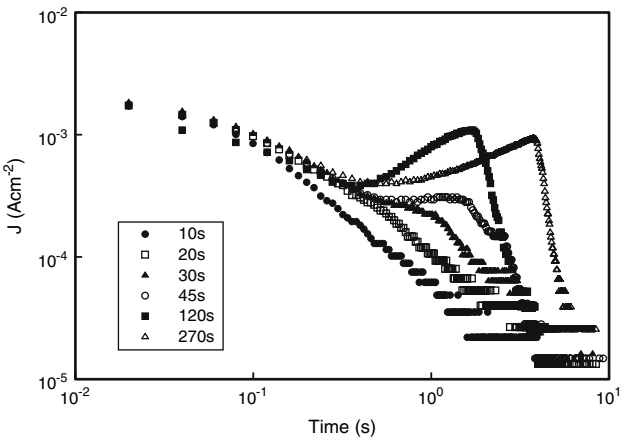

Fig. 5 Bleach currents recorded under ambient room temperature conditions for a 0.8 μm thick CMP electrochromic film using a PF_6^- counter-ion. The applied bleach voltage was $V_b = 2.0$ V. The colouration times that were used prior to bleaching are given in the inset legend

[1] Goldie DM, $\varepsilon_r = 3.2$ from unpublished capacitance data.

greater than about 45 s the current transients continue to display the strong signature overshoot previously observed for fully-coloured films in Fig. 1c. The extent of the current overshoot is progressively reduced as the colouration time is shortened and for colouration times below about 20 s have been rendered almost featureless in accordance with Eq. 2. A colouration time of around 20 s would thus appear to represent the critical threshold beyond which counter-ions start to occupy slow sites. The fraction of fast sites was therefore estimated by first integrating the $J(t)$ response in Fig. 5 for the colouration time of 20 s to calculate the amount of charge (0.46 mC cm^{-3}) that is held in fast sites. By comparing this charge with the total amount of collected charge held in both fast and slow sites for fully coloured films (3.50 mC cm^{-3}) the fraction of fast sites in the CMP film was calculated to be approximately 13%. Similar values are deduced when BF_4^- and ClO_4^- are used as summarised in Table 2. The calculated fraction of fast sites would appear to be too large, however, to be consistent with the deduced counter-ion mobility found in Fig. 3c where during the early stages of bleaching (at say $X1 = 0.01$ μm $\mu_i/\mu_F \approx 10^{-6}$. Early-stage bleaching in fully-coloured CMP films cannot therefore involve a mechanism whereby counter-ions are removed to the electrolyte via fast sites and these sites are immediately replenshied from slow sites as this would only allow a mobility increase by a factor of about $0.13^{-1} = 8$ from Eq. 9. The initial bleach period, which demands a rapid removal of counter-ion charge, must instead be accommodated by the removal only of counter-ions which initially occupy fast sites. Once this supply of counter-ions has been virtually exhausted, the remaining reservoir of counter-ions in slow sites will start to transfer to the now available slow sites to allow bleaching to continue. In this manner, the actual concentration of counter-ions held in fast-sites for $X1 = 0.01$ μm may assume a very small fraction of those that actually exist in the CMP film which allows μ_i/μ_F to assume the necessary small ratio from Eq. 9. Evidence to support the described early-stage bleach picture is provided in Fig. 5 where it is observed that for early times up to around 0.36 s the bleach currents follow a universal decay for colouration times which are sufficient to fully populate the fast sites. Integration of these universal current signals up to 0.36 s suggests that the early stage charge that is removed is around 0.28 mC cm^{-2} which compares favourably with the estimate of 0.46 mC cm^{-2} for the maximum charge fraction available from fast sites.

Conclusions

The bleaching mechanism in CMP electrochromic films is controlled by the removal of counter-ion charge from cross-linked colouration sites. Experimentally observed counter-ion bleach currents may be successfully described using a modified SCL model in which the counter-ion mobility increases as bleaching proceeds. It is suggested that the increase of counter-ion mobility may be associated with the transfer of counter-ions from colouration sites which have slow access times to those that have fast access times. Irrespective of the counter-ion type, the fraction of colouration sites in CMP films which have fast access is estimated to be around 14%, and the counter-ion mobility associated with these sites is about 5×10^{-4} cm^2 V^{-1} s^{-1}. The counter-ion size does, however, influence the transfer rate between slow and fast sites with fastest transfer occurring for smaller counter-ions.

References

1. Somani PR, Radhakrishnan S (2003) Mater Chem Phys 77:117
2. Lampert CM (2002) Glass Sci Technol 75:244
3. Rosseinsky DR, Mortimer RJ (2001) Adv Mater 13:783
4. Vondrak J, Sedlarikova M, Vlcek M, Mohelnikova K, Macalik M (2006) Mech Syst Mater Solid State Phenom 113:507
5. Lee ES, DiBartolomeo DL (2002) Solar Mater Solar Cells 71:465
6. Faughnan BW, Crandall RS (1980) Top Appl Phys 40:181
7. Monk PMS (1999) Crit Rev Solid State Mater Sci 24:193
8. Faughnan BW, Crandall RS, Lampert MA (1975) Appl Phys Lett 27:275
9. Crandall RS, Faughnan BW (1976) Appl Phys Lett 28:95
10. Mortimer RJ, Dyer AL, Reynolds JR (2006) Displays 27:2
11. Sonmez G (2005) Chem Commun 42:5251
12. Maud JM, Booth TW, Hepburn AR, Marshall JM (1990) In: Borissov M, Kirov H, Marshall JM, Vavrek A (eds) Proceddings of the 6th ISCMP. World Scientific, p 294
13. Goldie DM, Hepburn AR, Maud JM, Marshall JM (1993) Mol Cryst Liq Cryst 236:87
14. Hepburn AR, Goldie DM (1994) J Mater Sci Mater Electron 5:94
15. Bartlett ID, Hepburn AR (1995) Synth Met 70:1241
16. Bartlett ID, Marshall JM, Maud JM (1996) J Non-Cryst Solid 200:665
17. Lampert MA, Mark P (1970) Current injection in solids. Academic Press, New York
18. Mayer L, Melzer C, Barzoukas M, Fort A, Mery S, Nicoud JS (1997) Appl Phys Lett 71:2248
19. Street RA (1991) Hydrogenated amorphous silicon. Cambridge University Press, Cambridge